An Experimental Investigation of Stagnation-Point Injection

EDWARD A. BARBER JR.*
The Boeing Company, Seattle, Wash.

An experimental investigation of fluid injection at the stagnation point of a 1.25-in.-diam blunt body was performed in a 1-Mw plasma tunnel. The model was instrumented to measure average heat-transfer rates to the body by calorimetric means. Shock-wave standoff distances were measured from glow photographs. Nitrogen, helium, and hydrogen were used as injectants. The freestream Mach number varied between 6 and 8, and the total enthalpy was varied between 1700 and 4000 Btu/lb$_m$. The shock standoff distance fell into three distinct regimes, depending on the dissipation mechanism involved and the relative mass flow, and had a strong dependence on γ when correlated with the parameter, $FM_{12}^{1/2}$. The average nose heat-transfer data were correlated by this same parameter when the effect of hydrogen combustion was included.

Nomenclature

F = (ρV) wall/$(\rho U)_\infty$, relative mass flow
h_{wall} = static enthalpy at the wall
H = total enthalpy
M_1 = molecular weight of injectant
M_2 = molecular weight of freestream
M_{12} = ratio of M_1 to M_2
M_{jet} = exit Mach number of jet
M_∞ = freestream Mach number
$P_{T\infty}$ = total pressure of freestream
$P_{T\text{jet}}$ = total pressure of jet
$\dot{q}$ = average heat-transfer rate
R_n = body nose radius Reynolds number
S_T = Stanton number $\dot{q}/H\,\dot{m}_\infty$
S_{T0} = Stanton number, no injection
Δ_s = shock standoff distance
V = injection velocity
U = freestream velocity
ρ = density

Introduction

THE injection of mass into the boundary layer has long been considered as a possible means of protection of the noses of entry vehicles from high heat fluxes. Consideration has also been given to mass transfer, and stagnation-point injection in particular, to facilitate signal transmission by producing a region of low electron density in the shock layer covering a re-entry vehicle. Over the past few years mass addition has taken many forms including transpiration cooling, mass transfer cooling, and film cooling, to name the most important. These three methods have been reviewed in Ref. 1.

A number of investigators[2,3] have considered the problem of cooling by injection at the stagnation point. Warren[4] and McMahon[5] investigated the heat-transfer rate distribution on a hemispherical nose with helium and air injection. They found that the stagnation region was cooled locally by mass injection, but that downstream the injected flow reattached to the nose causing a stagnation ring or annulus that in some cases increased the total heat transfer to the nose.

Watt[6] was the first to examine the nature of the flow field caused by the interaction of a sonic jet of fluid directed upstream into a dissimilar supersonic stream. He managed to classify the regions in the interaction between the two jets (Fig. 1) by optical means. In the interaction region, a freestream must decelerate to zero velocity. If the freestream flow is supersonic and inviscid, this may only be accomplished through a shock wave. After passing through the shock wave, the flow may then decelerate through the subsonic region to zero velocity. The facing jet must also go through a similar process. Hence, the stagnation region consists of two supersonic fields separated by a subsonic field divided by a contact discontinuity, at which the stagnation point occurs. In the case of the subsonic jet, the decelerating shock of the jet is no longer required to describe the flow model, and the freestream decelerating shock and the contact discontinuity characterize the flow.

Romeo and Sterrett[7] recently made a study similar to Watt's, and they suggested a second decelerating mechanism, viscous dissipation, because two distinct types of jet interaction were observed. One occurred at low values of $P_{T\text{jet}}/P_{T\infty}$, the parameter used to describe the interaction, and was characterized by large shock standoff distances and conical

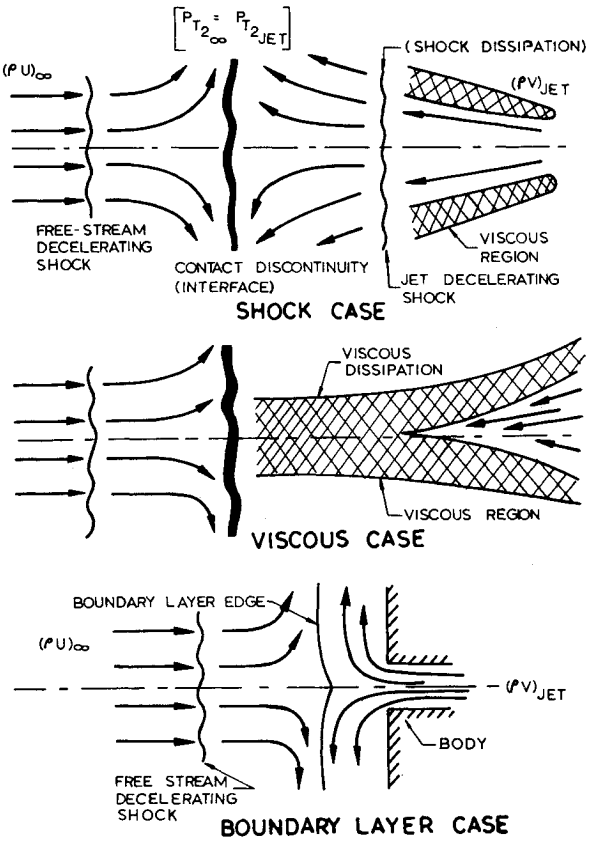

Fig. 1 Jet interaction regimes.

Presented as Preprint 63-433 at the AIAA Conference on Physics of Entry into Planetary Atmospheres, Massachusetts Institute of Technology, Cambridge, Mass., August 26–28, 1963; revision received March 16, 1965.

* Program Manager, Re-Entry Vehicle Section. Member AIAA.

common stagnation point must occur, and the flow in the shocks. Another occurred at higher mass flows and was characterized by reduced standoff distances and shock-wave shapes that resembled those associated with blunt bodies. The transition between the two flow states was abrupt and was shown to occur at various $P_{Tjet}/P_{T\infty}$ depending on body size and the jet exit Mach number.

The interface between opposed jets at the stagnation point is a contact discontinuity across which both static and stagnation pressures must be equalized. The ratio of the static pressure of the jet leaving the injection hole to the static pressure outside of the jet determines whether the jet is underexpanded or overexpanded. If the jet is overexpanded and the angle of expansion is greater than the angle of the viscous mixing occurring at the edge of the jet, the dissipation must occur by means of a shock at the point in the jet where it will produce the desired total pressure loss. If the jet is underexpanded, jet mixing may cause the dissipation to occur before a sufficiently large local jet Mach number is reached.

Bogdonoff[8] and others have studied the influence of a physical spike protruding from the stagnation point of a blunt body and the resulting heat transferred to the body. It was found that by separating the flow by use of a physical spike the average heat transfer to the body was appreciably reduced. In conceiving this investigation, it was envisioned that a combination of the advantages of mass transfer cooling and separation might be achieved which would result in an efficient and simple cooling system. Several investigations[9] have indicated that low molecular weight gases are potentially better coolants than high molecular weight gases; therefore, nitrogen, helium, and hydrogen were studied.

Test Description

The Boeing 1-Mw continuous (30 min) plasma tunnel has a conical nozzle that gives a Mach number of 6–8, depending on the total conditions of the arc chamber, and a total enthalpy capability of 1500–5000 Btu/lb$_m$ as determined by cooling-water calorimetry. Although crude, this method was the only one available for calibrating the energy density in the test section. (For a more detailed description of this general type of facility, the reader is referred to Ref. 10.) The test section was an 8-in.-diam free jet. The model was mounted on a water-cooled sting attached to an injection strut that allowed the model to be injected or retracted while the facility was in operation. The injection time of the model into the facility was on the order of 5 sec.

The model (Fig. 2a) was basically a water-cooled calorimeter. The temperature of the water was measured by two iron-constantan thermocouples suspended in the inlet and outlet channels. The water was circulated in the coolant chamber with the aid of turning vanes. The model was a 90° sector of a copper hemisphere, with a diameter of 1.25 in. and an injection orifice diameter of 0.101 in. The temperature of the injectant was monitored by an iron-constantan thermocouple suspended in the injectant tube. The coolant mass flow was measured by a Potter flow meter. Data ouputs were recorded on oscillographs. All measurements were made in a steady-state environment.

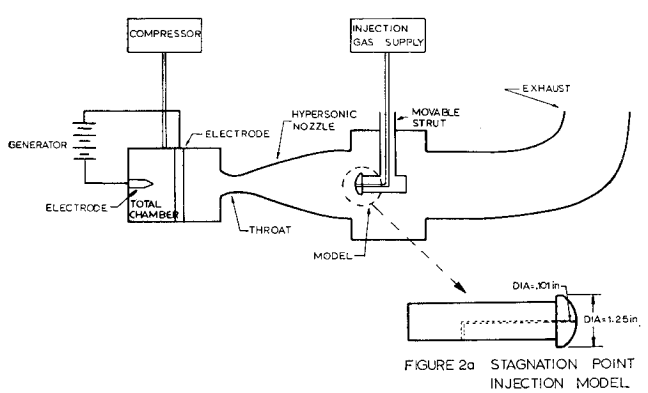

Fig. 2 Schematic drawing of Boeing plasma hypersonic wind tunnel.

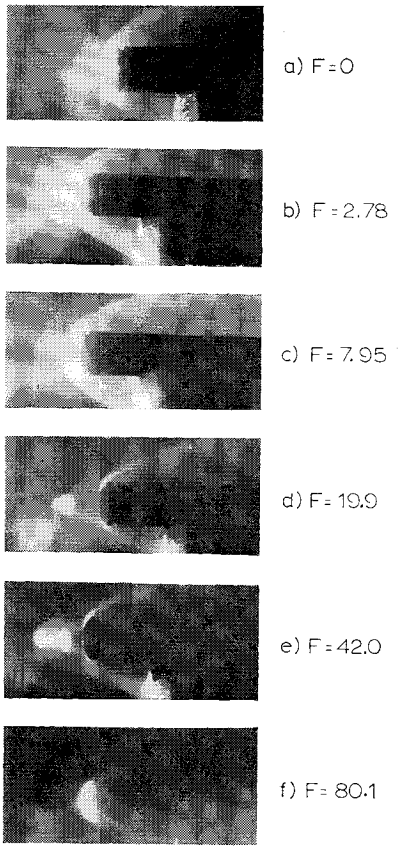

Fig. 3 Typical photographs of nitrogen injected at stagnation point, H_{total} = 4000 Btu/lb$_m$.

During the test the arc chamber was started and a steady flow established. The injectant was started while the model was in the retracted position, and the model was then injected into the stream. When steady-state measurements were attained for the initial test conditions, the injectant mass flow was changed to the next test point.

The nature of the arc-driven plasmajet is such that, in order to vary the average total enthalpy in the test section, the stagnation total pressure, and hence the mass flow, must also be varied because the electrical energy input to the stagnation chamber is held constant. The total enthalpy cannot be changed without a corresponding change in the freestream Reynolds number. At the higher enthalpies in this study the working fluid encounters severe dissociation and ionization. Preliminary investigation of this problem has indicated that the gas in the test section is probably in its frozen state. This conclusion is born out by the investigations of Harvey[11] in a similar facility.

The data taken were average heat-transfer measurements to the nose and glow photographs of the flow field caused by injection. This approach has given adequate results because of the radiant qualities of the shock layer at the temperatures at which the test was conducted.

Results

Shock Standoff Distance

Figure 3 shows typical glow photographs for nitrogen injection. The exterior edge of the shock layer was clearly discernible by the increased luminosity. Similarly the interface of the injectant layer and the shock layer was visible because of the sharp decrease in luminosity.

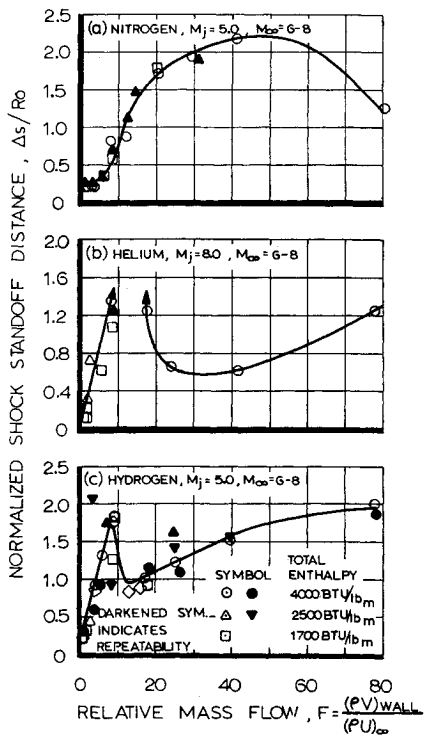

Fig. 4 Effect of blowing rate on shock standoff distance.

Measured shock standoff distances are given in Fig. 4, which shows that the parameter F, the relative mass flow, is fundamental in describing the flow. In Fig. 4a, for N_2, the three regimes of interaction are well defined. For $F < 3$ the shock standoff distances show little or no variation with increased mass flow. This regime corresponds to the case where the injected flow is retained within the boundary layer and does not disturb the inviscid shock wave or shock layer and will hereafter be called "boundary-layer regime." At relative mass flows greater than 3, the stagnation-point standoff distance increases proportionally with increases in relative mass flow until it reaches a maximum at $F \approx 40$. The shock standoff distance at $3 < F < 40$ is determined largely by viscous dissipation under the assumed flow model and hence will be termed the "viscous regime." An increase in F above 40 causes the shock standoff distance to decrease rapidly, corresponding to the transition from the viscous case to the large injection case that will be called the "shock regime" after its dissipative mechanism.

In Fig. 4b, for H_e, correlation through F is again shown, but the values of F at which the defining characteristics of the curve occur are different; this may indicate that F is not completely adequate to describe the flow field. Figure 4c, for H_2, shows that large injection rates increase the shock standoff distance in the shock regime to a value as large as that achieved in the viscous regime.

Lam[12] has indicated that the interface is characterized by the quantity $F\epsilon_i^{1/2}$ where ϵ_i is the density ratio across the interface. The contributions to ϵ_i are primarily from the molecular weight of the gas and the density ratio across the jet-decelerating shock. Figure 5 shows the standoff distances for all three injectants correlated by products of the relative mass flow F and the square root of the ratio of the molecular weights of the gases $M_{12}^{1/2}$. The correlation appears to be successful for the nitrogen and hydrogen gases but not for helium. The slope of the data is different in the viscous regime, and the level is different in the shock regime. The obvious difference between the two curves is in γ because helium is a monatomic gas whereas nitrogen and hydrogen are diatomic gases. The density ratio across the jet-decelerating shock is a function of γ, and the exit Mach number of the jet depends on γ. The jet exit Mach number establishes whether the jet is overexpanded or underexpanded, which in turn determines which of the dissipation mechanisms will be dominant. The flow in the shock regime appears to be a stronger function of γ than that in the viscous regime. The standoff distances for $F > 60$ vary by as much as a factor of 3.

Average Heat-Transfer Rates

As noted previously, the energy density in the stream is varied by changing the mass flow of the tunnel. A suitable nondimensionalization of the heat-transfer rate is made by forming the following nondimensional group: $S_T/S_{T0} \approx (q/H)/(q/H)_0$. Implied are the facts that $H \gg h_{wall}$ and $P_r = 1$. The heat-transfer data are shown in this form in Figs. 6 and 7. Note that in each case the data have been consolidated by the nondimensionalization even though it is for different free-stream mass flows.

Consider the case of nitrogen injection (Fig. 6a). As the injection rate increases initially from zero, the heat-transfer rate decreases rapidly. Further increase in F causes the heat-transfer rate to increase to values above those for no mass transfer. This is an unexpected phenomenon, but close examination of Fig. 3 shows a visible reattachment or stagnation ring that is annular in shape. The increased size of this stagnation region over the zero injection stagnation point may well explain the unexpected increase in average heat-transfer rate.

We may infer the upper limit of the boundary-layer regime from the heat-transfer measurement, since the increase in heat transfer due to injection seems to come from the interference of the shock layer by the jet. This is precisely the condition that was established as a criterion for the limit of the boundary-layer flow. However, this limit is only valid for the orifice configuration used in this test; it would vary with orifice diameter. Thus, the low mass injection regime mentioned earlier has also been defined in terms of heat-transfer measurements and is seen to occur at $0 < F < 3$, which agrees with previous conclusions based on the shock standoff distance measurements.

Maximum heat transfer occurs at $F \approx 8$ and amounts to a 10% increase as compared to $F = 0$. A re-examination of Fig. 4a indicates that this maximum in heat-transfer rate does not correspond to any well-defined point on the shock standoff curve. Again, by observing the photographs, the reduction from the heat-transfer maximum may be seen to occur as the stagnation annulus moves away from the cooled stagnation

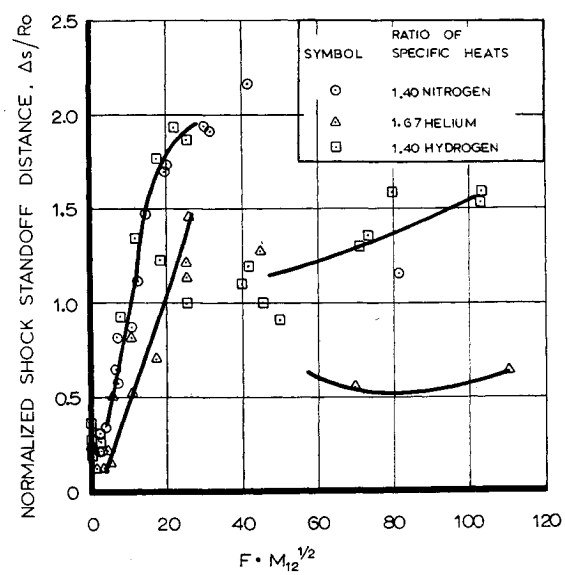

Fig. 5 The effect of molecular weight on shock standoff distance.

region. The region downstream of the stagnation annulus is dominated by the attached shock layer and contributes the largest portion of the heat transferred to the body. As the injectant rate was further increased, the stagnation annulus moved off the body, and the heat transfer to the body approached zero.

In Fig. 6b for helium, the heat transfer again peaks at low injection rates; however, the decrease now occurs at even lower values of F. The data taken in this range of F appear to be insufficient to define the limits of the boundary-layer regime for helium injection. The reduction in heat transfer after the maximum is monotonic and exhibits no discernible characteristic at the point where the discontinuity in shock standoff distance occurred. As expected, helium is a more efficient coolant than nitrogen.

As hydrogen (Fig. 7) was injected into the stagnation region, the heat-transfer rate increased almost immediately by 65% of the zero mass injection value. Subsequent increases in the injection parameter resulted in decreases in the heat-transfer rate, approaching zero as the shock layer was completely separated from the body. A comparison between the hydrogen and the helium injection cases indicated that the hydrogen data were roughly 60% higher for all mass transfer rates when the effect of molecular weight was considered. It is concluded that combustion occurred within the hydrogen-air interface and contributed to the heat transferred to the body. Unfortunately, the combustion of hydrogen is not a visible phenomenon, and the glow photographs offer no assistance in locating the reaction zone.

Hartnett and Eckert[13] calculated the effects of combustion at the stagnation point of a blunt body with hydrogen injection. The dashed curve in Fig. 7 was obtained from their

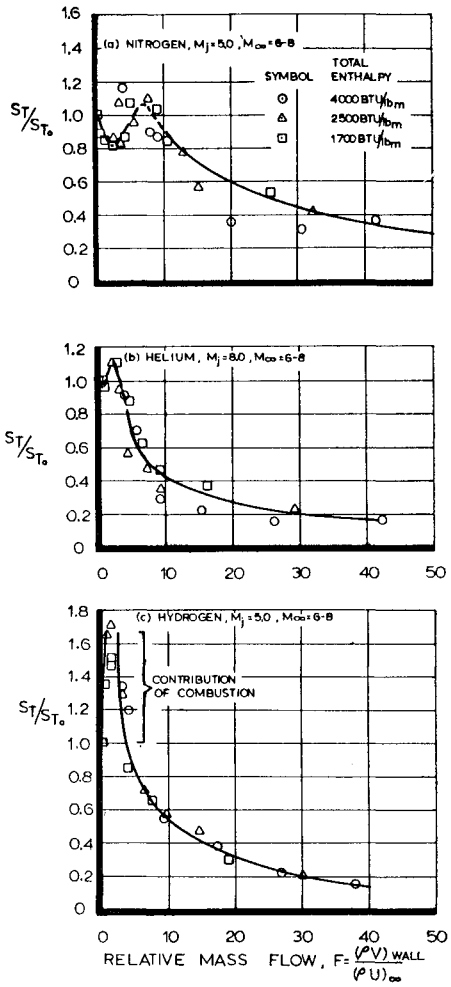

Fig. 6 Effect of blowing rate on heat transfer.

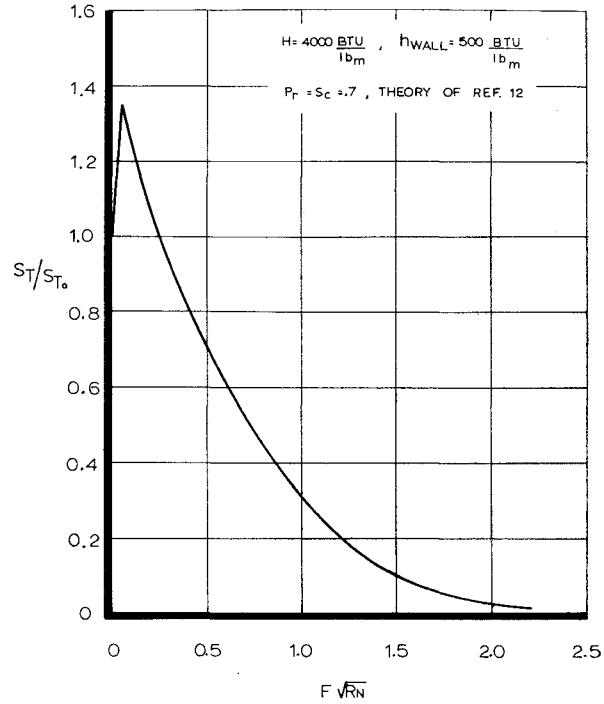

Fig. 7 Stagnation-point transpiration with hydrogen, boundary-layer theory.

calculations. Although the theory indicates an increase in heat-transfer rate of approximately 45%, the data from this study indicate an increase of approximately 65%. Three possible explanations for this discrepancy follow:

1) The theoretical curve is for $h_{wall} = 500$ Btu/lb$_m$, and the experimental wall enthalpy, although unknown, is probably an order of magnitude less. Thus, the experimental heat transfer would be expected to be larger.

2) The helium and nitrogen data indicated an increase in heat-transfer rate that has been attributed to interaction of the jet with the inviscid flow. This may also be occurring in the case of hydrogen injections.

3) The theory is for diffuse injection, whereas the experiment illustrates discrete injection. Figure 8 shows a correlation of average heat-transfer rates for the three different types of injectants with the parameter $M_{12}^{1/2}$. Here the combustion effects are assumed to be 65% of S_T/S_{T_0} at all mass flows. (Hartnett and Eckert assumed S_T/S_{T0} due to combustion to be constant for large injection rates.) The correlation is quite satisfactory considering the fact that three enthalpies, three injectants, and many freestream and injectant mass flows are represented.

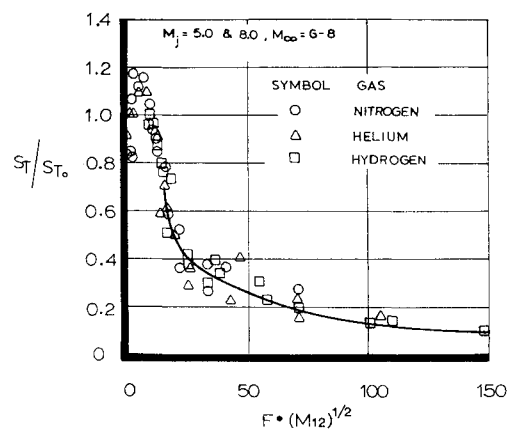

Fig. 8 Effect of molecular weight on heat transfer.

Conclusions

The effects of mass injection at the stagnation point of a blunt body fall naturally into the three regimes of flow interaction:

1) Boundary-layer regime. The injected flow does not disturb the inviscid shock layer or shock wave and is contained within the boundary layer. The upper limit of this regime occurs at $F \approx 3.0$ for the configuration investigated in this study.

2) Viscous regime. The jet pierces the body shock, and large shock standoff distances on the order of the body diameter may be realized. The dissipative mechanism that allows the jet stagnation pressure to equal the shock-layer stagnation pressure at the interface is viscous, and a greater jet length is required for the adjustment in stagnation pressure to occur. This condition is usually associated with an underexpanded jet.

3) Shock regime. An abrupt transition from the viscous regime occurs when the ratio of the jet pressure to the jet exit pressure becomes large enough so that the jet expansion is the same order as the growth of the viscous mixing layer surrounding the jet. This transition is accompanied by a severe decrease in shock standoff distance and the occurrence of a normal shock as the dissipative mechanism. The shock wave is more efficient than the viscous mechanism, and the adjustment to the shock-layer stagnation pressure is more rapid.

The shock standoff distance exhibits a well-defined dependence on the ratio of specific heats of the injectant, as well as its molecular weight. The average heat-transfer rate decreases in the boundary-layer regime for noncombustible gases and increases rapidly for combustible gases. Hydrogen injected into the boundary layer causes additional energy to be released to the body by combustion, causing increases to the body heat transfer of approximately 65% at the test conditions in this investigation. This measurement agrees qualitatively with calculations of Ref. 14.

The average heat-transfer rate increases 10% above the no injection case at mass injection rates corresponding to $F = 5$ for noncombustible gases. This is attributed to the occurrence of a stagnation ring or annulus that increases the local heat transfer in the vicinity of the stagnation ring.

At large mass transfer rates the shock layer separates from the body, and the corresponding average heat-transfer rate approaches zero. This occurs primarily in the shock regime.

The average heat-transfer rate to a body protected by a jet of gas directed into the oncoming stream may be correlated satisfactorily on the bases of the parameter $FM_{12}^{1/2}$, if the contributions of combustion are considered.

References

[1] Leadon, B. M., "The status of heat transfer control by mass transfer for permanent surface structures," *Proceedings of AFOSR Conference on Aerodynamically Heated Structures*, edited by Peter E. Glaser (Prentice-Hall Inc., Englewood Cliffs, N. J., 1962), pp. 171–196.

[2] Hayday, A. A., "Mass transfer cooling in a steady laminar boundary layer near the stagnation point," *Proceedings of Institute of Heat Transfer and Fluid Mechanics* (Stanford University Press, Stanford, Calif., 1959).

[3] Baron, J. R. and Scott, P. B., "The laminar boundary layer with external flow field pressure gradients," Massachusetts Institute of Technology TR 419 (December 1959).

[4] Warren, C. H. E., "An experimental investigation of the effect of ejecting a coolant gas at the nose of a bluff body," J. Fluid Mech. **8**, 400–417 (1960).

[5] McMahon, H. M., "An experimental study of the effect of mass injection at the stagnation point of a blunt body," California Institute of Technology, Guggenheim Aeronautical Lab., Hypersonic Project Memo 42 (1958).

[6] Watt, G. A., "An experimental investigation of a sonic jet directed upstream against a uniform supersonic flow," Institute of Aerophysics, Univ. of Toronto TN 7 (January 1956).

[7] Romeo, D. J. and Sterrett, J. R., "Exploratory investigation of the effect of a forward-facing jet on the bow shock of a blunt body in a Mach number 6 free stream," NASA TND-1605 (February 1963).

[8] Bogdonoff, S. M. and Vas, I. E., "Preliminary investigation of spiked bodies at hypersonic speeds," Princeton Univ. Aeronautical Engineering Rept. 412 (March 1958).

[9] Gross, J. F. et al., "A review of binary boundary layer characteristics," Rand Corp. RM-2516 (June 1959).

[10] "Boeing 1–2 megawatt hypersonic plasma tunnel calibration data," The Boeing Co. Report.

[11] Harvey, J. K. and Simpkins, P. G., "A description of the Imperial College arc-heated wind tunnel," J. Roy. Aeron. Soc. **66**, 637–641 (October 1962).

[12] Lam, S. H., "Interaction of a two-dimensional inviscid incompressible jet facing a hypersonic stream," Air Force Office of Scientific Research TN 59-274, Princeton Univ. (March 1959).

[13] Hartnett, J. P. and Eckert, E. R. G., "Mass transfer cooling with combustion in a laminar boundary layer," Heat Transfer and Fluid Mechanics Institute, Stanford Univ. (1958).

[14] Ferri, A. and Bloom, M. H., "Cooling by jets directed upstream in hypersonic flow," Wright Air Development Center TN 56-382 (May 1957).